Article

The Influence of the Abduction Joints of Four Fingers to Grasp: Experimental and Simulated Verification

Yadong Yan [1], Chang Cheng [2], Mingjun Guan [1], Jianan Zhang [1] and Yu Wang [1],*

[1] School of Biological Science and Medical Engineering, Beihang University, Beijing 100191, China; adam7217@buaa.edu.cn (Y.Y.); sy1910110@buaa.edu.cn (M.G.); baby0303zjn@buaa.edu.cn (J.Z.)

[2] Department of Mathematics and Computer Science, Colorado College, Colorado Springs, CO 80903, USA; d_cheng@coloradocollege.edu

* Correspondence: wangyu@buaa.edu.cn

Abstract: The thumb is the most important finger of the human hand and has a great influence on grasp manipulations. However, the extent to which joints other than the thumb joints affect the grasp, and thus, which joints should be included in a prosthetic hand, remains an open issue. In this paper, we focus on the metacarpophalangeal joints of the four fingers, except the thumb, which can generate flexion/extension and abduction/adduction motions. The contribution of these joints to grasping was evaluated in four aspects: grasp size, grasp force, grasp quality and grasp success rate. Six subjects participated in experiments with respect to the maximum grasp size and grasp force. The results show that possessing abduction mobility of the metacarpophalangeal joints can increase the grasp size by 4.67 ± 1.93 mm and the grasp force by 5.27 ± 4.25 N. Then, the grasping quality and success rate were tested in a simulation platform and using a robotic hand, respectively. The results show that grasp quality was promoted by 76.7% in the simulated environment with abduction mobility compared to without abduction mobility, whereas the grasp success rate was promoted by 68.3%. We believe that the results of this work can benefit the understanding of hand function and prosthetic hand design.

Keywords: metacarpophalangeal joint; prosthetic hand design; grasping evaluation

1. Introduction

The human hand is a highly complex masterpiece with 23 degrees of freedom (DOF) [1,2] (Figure 1a). The thumb, which has three joints and 5 DOFs, plays a vital role in the functional integrity of the human hand and has been widely studied [3–5]. The other four fingers each have three joints and 4 DOFs. These joints can be named the distal interphalangeal (DIP) joint, proximal interphalangeal (PIP) joint, and metacarpophalangeal (MCP) joint, respectively, from fingertip to bottom. The DIP and PIP joints are 1-DOF joints, while the MCP joints are 2-DOF joints with a condyloid shape, which enables a large workspace of the fingers [6]. However, the contribution of this type of joint to grasp manipulations is rarely studied, and in developing a prosthetic hand, the dexterity of the MCP joints is frequently ignored. Relevant research has focused on the mechanical and kinematic properties of MCP joints. Sprague et al. analytically and experimentally investigated the kinematic behavior of the human MCP joint [7]. Then, they analyzed the biomechanical characteristics of MCP joint prosthesis design with fresh cadaver finger rays in later work [8]. Yuan et al. analyzed the move independence of the MCP joint by a series of grasp experiments and hand gestures [9]. Vinjamuri et al. presented time-varying synergies that were observed during reach and grasp experiments in angular velocity profiles of MCP joints and PIP joints in [10]. However, these works only studied the characteristics of the joint itself and did not take the task into consideration.

The grasping operation is a critical aspect in evaluating the impact of joints on the human hand. Halil et al. analyzed the load distribution and contact area in four common

grasp types used in daily living activities, and the results demonstrated that the surface of the MCP joint was one of the main components of the maximum contact area [11]. Federico et al. explored the actual contribution of independent fingers while performing activities of daily living, including grasping different objects under three hand configurations achieved using custom built orthoses [12]. The results suggested that the remarkable grasping skills of the human hand rely more on the independent abduction/adduction (ab/d) of the MCP joints than on their independent flexion/extension (flex/ex). Mohamed et al. evaluated the correlations of coordinated movements in human hands during 23 grasp tasks, and they found that the ab/d motion of the hand fails to show either strong coordination or group coupling with other joint movements [13]. In this study, we mainly expanded the research in two aspects: (1) the constraint condition of MCP joints is further divided into four different situations for research, and (2) we explore multiple aspects of grasping, namely grasping size, grasping force, grasping quality and grasping success rate.

In general, in the development of prosthetic hands, a key point is the number of active DOFs that the hand has, which means the number of actuators. Some robotic hands have achieved a high number of DOFs close to the human hand, such as the Shadow Hand [14], and the Anatomically Correct Testbed Hand (ACT hand) [15]. However, these prosthetic hands are expensive, weighty, and sophisticated in design and control. Therefore, there is often a trade-off between complexity and accessibility in most scenarios of hand design, such as the most advanced commercially available prosthetic hands (Bebionic Hand, i-Limb Hand, and Michelangelo Hand) [16,17]. These hands have only 5–6 active DOFs with the four fingers that can merely produce flex/ex motion; namely, the MCP joints of these hands are 1-DOF joints [18]. Similar circumstances can be seen in the design of most anthropomorphic soft robotic hands, such as [19–24]. The MCP joints of these soft hands are all 1-DOF joints incapable of producing ad/b motion. Some exceptions of reducing hand DOFs are given as follows: Xu et al. proposed a highly biomimetic robotic hand in which the MCP joints of the index finger and middle finger have ab/d DOF, while the ring finger and little finger do not [25]. Ficuciello et al. developed an underactuated hand with EMG/voice-based multimodal control, and it has two ab/d DOFs distributed in the index finger and little finger separately [26]. The BionicSoftHand by Festo has one single ab/d DOF lying in the index finger [27]. In conclusion, it is still an open question as to which DOFs are most indispensable in the hand and which are relatively unimportant. Omitting the ab/d DOF of MCP joints is not necessarily the most suitable approach to prosthetic hand design.

In this paper, we explore the influence of ab/d DOF of MCP joints on grasping by human hand experiments and simulation. Intuitively, the grasp action of the human hand varies according to the object shape and hand gesture [28]. Previous work has divided grasps into three main types: power grasp, intermediate grasp and precision grasp [29,30]. Cini et al. demonstrated that the precision grasp is the most commonly used grasp type, accounting for 62% of grasp operations [31]. Hence, in this work, we concentrate on the precision grasp in which only the distal and intermediate phalanges are used.
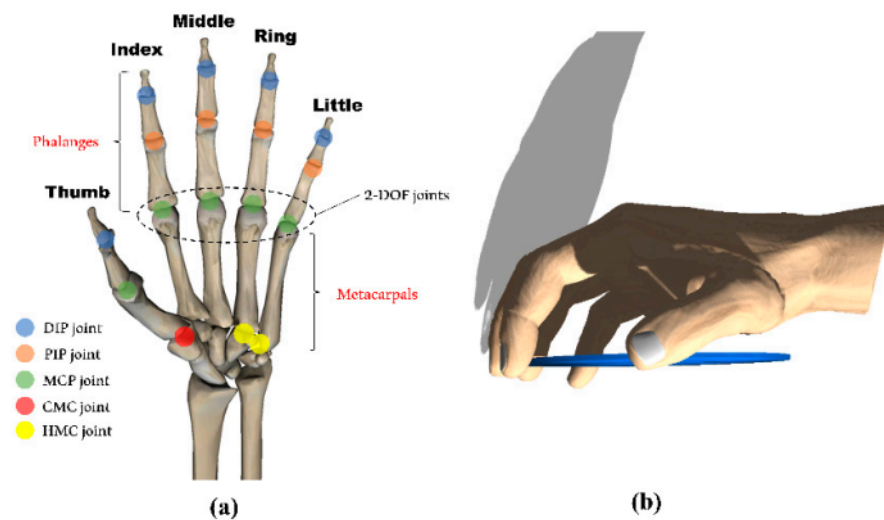
Figure 1. (**a**) A skeletal joint model of the human hand; (**b**) the grasp type used: precision disk [30].

2. Materials and Methods

We evaluated the grasp size, grasp force, grasp quality and grasp success rate under the four types of constraint conditions of ab/d DOFs. The objects were a series of disks with varied diameters. Accordingly, the grasp type used in all experiments in this study is *precision disk* from [30] (Figure 1b). The grasp size and grasp force were tested by human subjects experimentally. The grasp quality, which was hard to quantify in real grasping, was measured in a simulator. Then, we tested the grasp success rate using a soft robotic hand. In this section, the setup and process of these experiments and simulations are demonstrated in detail.

2.1. Constrained Conditions of ab/d Joints

First, we divided the distribution of ab/d DOF of MCP joints into four types:

(1) All four fingers have ab/d DOF, namely, the hand is free (Free);
(2) Only the ring finger and little finger have ab/d DOF, namely, the ab/d DOF of the index finger and middle finger are locked (IM-L);
(3) Only the index finger has ab/d DOF, namely, the ab/d DOF of the middle finger, ring finger and little finger are locked (MRL-L);
(4) None of the four fingers had ab/d DOF, namely, the index finger, middle finger, ring finger and little finger were locked (IMRL-L).

Two factors were taken into consideration for the classification: one is the existing robotic hand design mentioned above, and the other is that the middle finger was actually regarded as the central axis of the hand during the naturally fan-shaped opening of the hand [32].

2.2. Design of the Joint Restrictor

To achieve the constraint condition of ab/d joints, a joint restrictor was developed, as shown in Figure 2a. It consisted of up to 4 finger rings with a thickness of 0.5 mm connected by connecting strips. There were evenly distributed small holes on the strips to adjust the distance between the rings. The size of each part of the restrictor is customized by the hand size of each subject. *L*1, *L*2, and *L*3 are the distances between adjacent fingers. *D*1, *D*2, *D*3, and *D*4 are the diameters of the index finger, middle finger, ring finger, and little finger, respectively. The rings of the index finger, middle finger, and ring finger are aligned in the vertical direction while the ring of the little finger is lower than them. It is an anatomical design, and the distance between the ring of the little finger and other rings in

the vertical direction is *H*. The restrictor worn by each subject was customized according to the measurement of their hands. The hand size of each subject is shown in Table 1.
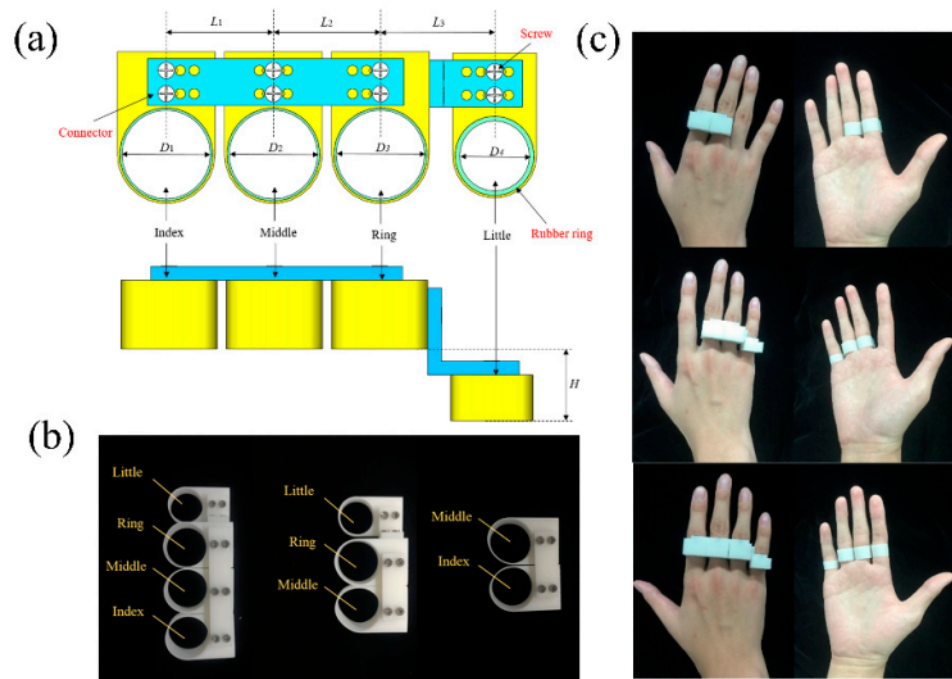

Figure 2. The ab/d DOFs restrictor. (**a**) Parameter definition, (**b**) three types of restrictors, (**c**) a human hand wearing the restrictor.

Table 1. Parameters of the hands of the subjects.

	Age	Gender	L1	L2	L3	D1	D2	D3	D4	H	Hand Length	Hand Strength
Subject 1 (S1)	24	M	22.3	20.4	20.1	19.2	18.3	18.3	17.2	8.2	188	48.33
Subject 2 (S2)	26	M	20.8	20.6	20.9	19.1	18.4	18.4	16.5	7.4	187	65.42
Subject 3 (S3)	21	M	21.5	20.0	20.5	17.5	17.9	17.2	15.7	8.2	170	73.28
Subject 4 (S4)	29	M	22.5	21.4	20.0	19.3	19.4	18.9	18.0	9.8	162	62.0
Subject 5 (S5)	30	F	20.0	19.6	19.5	17.8	17.6	16.4	14.2	5.6	156	43.8
Subject 6 (S6)	38	F	22.5	20.5	19.3	17.8	17.5	16.5	15.2	6.4	164	61.63

M, male; F, female; unit of the first 9 parameters after gender is mm and of the hand strength is N.

There are three types of restrictors according to the four types of constraints of ab/d DOF (Figure 2b): The first constraint can limit the ab/d motions of all four fingers; the second constraint can limit the ab/d motions of the index finger, middle finger, and ring finger; and the third constraint can limit the ab/d motions of the index finger and middle finger. By wearing it (Figure 2c), the ab/d DOF of the corresponding finger was locked, but all of the fingers could still flex to grasp. It should be noted that the restrictor also limits the separate bending of the fingers, leading to a coupled bending motion. Since the grasp type used in this study is *precision disk*, which does not require the fingers to bend alone, the coupling of bending is acceptable. In addition, during the experiments, the objects can still produce a small range of abduction movements of no more than 5 degrees due to material deformation after wearing the restrictor. It is small compared with normal abduction, which is acceptable. The restrictor was made of 3D printing resin material with a very light weight, and the heaviest one was 19 g.

2.3. Grasping with the Human Hand

Six able-bodied subjects (2 females and 4 males, age range 21–38 years, see Table 1) participated in this study. Informed consent according to the Declaration of Helsinki was obtained before conducting the experiments for each subject. Eligible subjects fulfilled the following inclusion criteria: (i) age between 20 and 40 years, (ii) body mass index (BMI) between 18.5 and 24, and (iii) full hand function. Subjects were recruited in the area of Beijing and screened during a first visit in which they were instructed on the testing procedure.

2.3.1. Grasp Size by Disk-Tower Test

A series of hand function tests were proposed for specific purposes [33,34]. However, most of them are designed for functional rehabilitation training and testing of the disabled. In this study, we designed a platform to test the hand grasping ability, as shown in Figure 3, which is named the disk-tower test (DTT). There are two circles on the platform, the base circle and the target circle. At the beginning of the test, 46 polylactic acid (PLA) disks were placed on the base circle, all with a thickness of 10 mm. The maximum diameter of the disk at the bottom is 190 mm, and the diameter of the disk decreases by 2 mm from the bottom to the top, shaped like a tower. The top disk is 100 mm in diameter. The subjects needed to grasp the disks on the base circle from top to bottom in turn and put them on the target circle one by one. Then the diameter of the disk at the bottom of the target circle is the smallest, and the diameter of the disk at the top is the largest, shaped like an inverted tower. When the subjects could not grasp the disk or the disk tower on the target circle collapsed, the trial was over. Then, the diameter of the last successfully placed disk was recorded. During the test, subjects needed to grasp every disk with a *precision disk* gesture, and the palm was horizontal; namely, a pinch grasp was not allowed. The hand was not allowed to touch any disk except when grasping during the test.
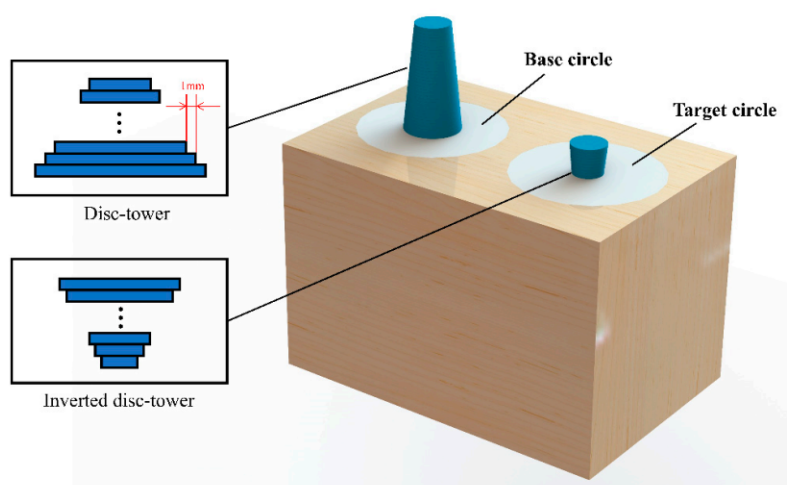

Figure 3. Outline of the disk-tower test.

Every subject was tested under four constrained conditions of ab/d DOFs by wearing three different restrictors and without restrictors. Three trials for each condition and a total of 12 trials were conducted for every subject. The results in each condition were averaged to determine the grasp size. Considering that hand size is a nonnegligible factor in the test, the grasp size was then normalized by dividing the hand length. The hand length is the distance from the wrist to the middle fingertip, which was measured before the experiments and is shown in Table 1.

2.3.2. Grasp Force

The effect of ab/d DOFs on the grasp force was tested experimentally. The setup is shown in Figure 4. A disc was fixed on the top of the digital force meter. A linear guide was used to adjust the height of the disk to enable the arm of the subject to be parallel to the ground so that they could grasp the disk only by arm strength. For each trial, the subject was asked to grasp the disc with a *precision disk* gesture and try their best to lift the disc. The maximum force in the process was recorded as the grasp force. A set of disks increasing in diameter with a gap of 10 mm was employed according to the DTT results in this experiment. The diameter of the smallest disk was 100 mm, and the diameter of the largest disk was smaller than the minimum grasp size in the DTT for each subject. Under four constraint conditions (Free, IM-L, MRL-L, and IMRL-L), the subjects needed to try each disk three times separately, and the results were averaged as the grasp force. For six subjects, a total of 504 trials were obtained in this experiment.
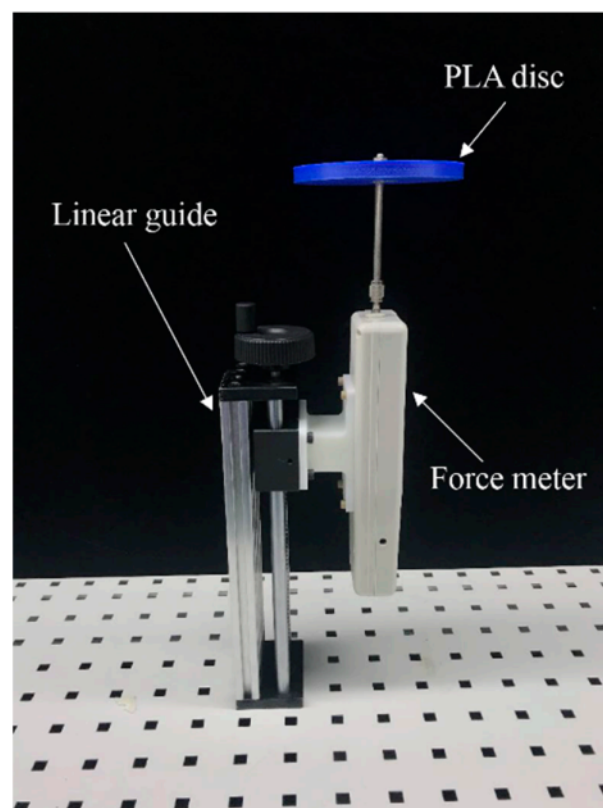

Figure 4. Setup of the grasp force experiments.

Similarly, the grasp force was normalized by dividing the hand strength. The hand strength shown in Table 1 was defined as the force of lifting a cylinder with a diameter of 50 mm using the same setup.

2.4. Grasping with a Simulator

In this subsection, we explored the effect of ab/d DOF on grasp quality. In general, most grasp quality metrics were proposed based on the locations of the contacts between the hand and the target object, which were hard to measure in a real environment. Hence, we used "GraspIt!", a publicly available grasp simulator developed by Matei and Peter [35–37], to evaluate the grasp quality. This simulator has a robotic hand library, including a human hand model with 20 DOFs. Users can import objects for grasp planning and analysis with a built-in simulated annealing algorithm [38]. A grasp quality function was defined as formulations (1) and (2) [37]. A set of desired contact points was predefined of a certain hand model. For the human model used in this experiment, the point number is 18 identified by the

index i. $\hat{n}_i$ and o_i are the normal and distance between the desired contact point of the hand model and the object, respectively. α is a scaling parameter, and Q is the value of the quality function for a given grasp. All Q values are higher than zero and a higher value indicates a higher grasp quality. The simulator GraspIt! takes into account factors such as gravity, friction, torque, collision, and so on, which can simulate the physical environment in the real world very realistically, so it is adopted.

$$ffi_i = \frac{o_i}{\alpha} + \left(1 - \frac{\hat{n}_i \cdot o_i}{|o_i|}\right) \tag{1}$$

$$Q = \sum_{\substack{\text{all desired} \\ \text{contacts}}} (1 - ffi_i) \tag{2}$$

In this simulation experiment, the virtual constraint was added to the human hand model, and four different constraint hand models corresponding to the ab/d DOF types defined in Section 1 were used. We imported six disks with a diameter between 110 mm and 160 mm with an interval of 10 mm into the simulation space and used the simulated annealing algorithm to plan the grasp. The thickness of all disks was 10 mm. According to [37], the simulated annealing algorithm starts to converge after 60,000 iterations. Therefore, the number of iterations for each planning was set to 70,000, and the grasp gestures with the highest quality were recorded. For each constraint hand mode, the grasp was planned 10 times for each disk size, and a total of 240 ideal grasping postures were obtained in this experiment.

2.5. Grasping with a Soft Robotic Hand

One of the purposes of this study is to provide an experimental basis for the design of robotic hands. In this subsection, a soft five-fingered robotic hand with ab/d DOFs of the fingers based on our previous work [39] was adopted to evaluate the grasp success rate, as shown in Figure 5. The robotic hand used was tendon driven. The MCP joints were composed of two perpendicular notched continuum structures (Figure 5a), so each finger had two tendons to produce flex/ex and ab/d motions.
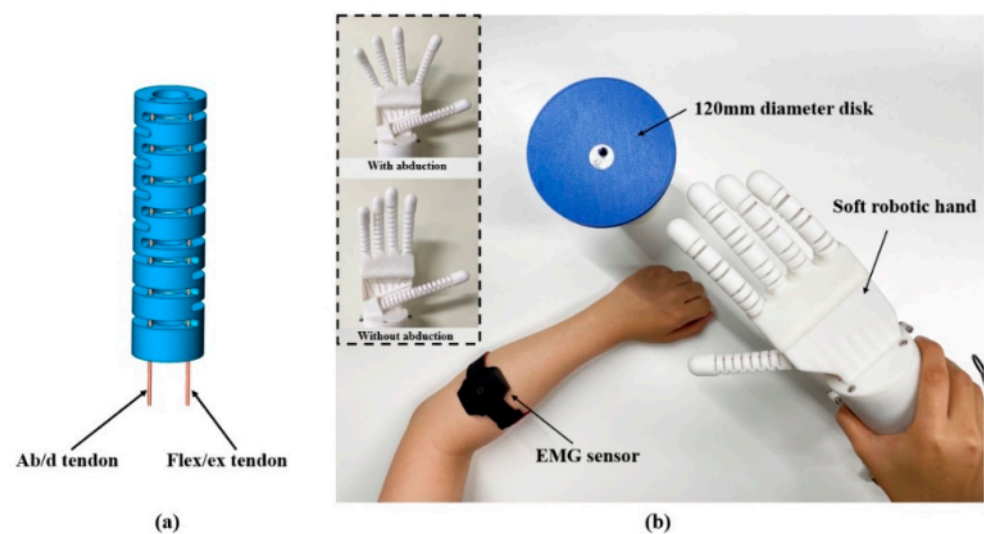

Figure 5. The soft robotic hand used to evaluate the grasp success rate. (**a**) The two-DOF MCP joint; (**b**) grasping a 120 mm diameter disk with a soft robotic hand. Left: two pregrasp gestures.

In this experiment, subjects were asked to grasp a disk with a diameter of 120 mm using the soft robotic hand. Two pregrasp gestures were defined: one was hand open without finger abduction, and the other was hand open with the four fingers abducting

(Figure 5b). The subject needed to first adjust the soft hand to an adequate position and gesture and then control the soft hand to execute the programmed grasp through the surface electromyography (sEMG) sensor attached to their arm. A simple threshold controlling method was used to trigger the grasp motion. After this, the subject needed to lift the disk to a certain height and sway the soft hand. If the disk did not fall or slide, the grasp was successful; otherwise, it failed. Each subject performed ten attempts using two pregrasp gestures, and the success rate was recorded.

3. Results

3.1. Grasping with the Human Hand

3.1.1. Grasp Size

The experimental results of DTT are shown in Figure 6a, which shows that all subjects had the smallest grasp size under the IMRL-L condition and the largest grasp size under free conditions, with an increase of 4.67 ± 1.93 mm. The most significant gap is 7.33 mm (S2). Defining the grasp size under the free condition as the baseline, the average difference between it and the grasp size under the IM-L, MRL-L, IMRL-L conditions are 0.78 mm, 1.67 mm, and 4.67 mm, respectively. It should be noted that there were two identical cases: the grasp sizes of S1 under the Free and MRL-L conditions were both 183.33 mm; and the grasp sizes of S4 under the Free and IM-L conditions were both 168 mm. This can be explained by the fact that when grasping a disk, at least three fingers are usually used to contact to gain a balanced state. Therefore, there is still at least one finger (except the thumb and the middle finger) to abduct to form a larger grasp workspace under IM-L and MRL-L conditions. Figure 6b shows the normalized grasp size, which was evaluated using the Wilcoxon test, and the results are shown in Table 2. There was a significant difference between the free condition and the IMRL-L condition.
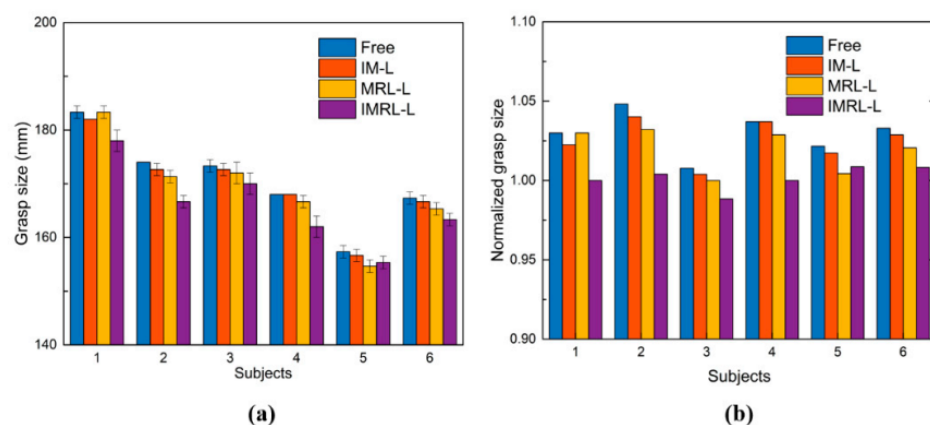

Figure 6. Results of the disk-tower test. (**a**) Grasp size, (**b**) normalized grasp size.

Table 2. Results of Wilcoxon test.

		IM-L versus Free	MRL-L versus Free	IMRL-L versus Free
Grasping with human hand	Normalized grasp size	$p = 0.335$	$p = 0.619$	**$p = 0.009$ ***
	Normalized grasp force	$p = 0.335$	$p = 0.295$	**$p = 0.039$ ***
Grasping with simulator	Average grasp quality	$p = 0.3095$	$p = 0.0931$	$p = 0.0649$
Grasping with robotic hand	Success rate	——	——	**$p = 0.0043$ ***

* Significant results.

3.1.2. Grasp Force

The experimental results of the grasp force under four conditions are shown in Figure 7. Figure 7a shows that the grasp force of all subjects basically decreases with increasing the disk diameter. For all disks, the average grasp force under the free condition is largest, while that under the IMRL-L condition is smallest, with a gap of 5.27 ± 4.25 N. The differences between the free condition, the IM-L condition and the MRL-L condition are comparatively small, which are 3.10 N and 3.95 N, respectively. It should be noted that for S1, the grasp forces of the disk with a diameter of 110 mm are larger than those of the disk with a diameter of 100, which might result from when the disk is relatively small, the variation of the disk diameter is not significant for the grasp force. We can see that as the diameter increases further, the decreasing trend of the grasp force is more prominent. Figure 7b shows the frequency distribution histogram of the normalized grasp force under four conditions. The frequency distribution in the range of 0.8 to 1 is the highest under the free condition. As the number of restricted ab/d DOFs increases, the frequency distribution inclines to a lower range. The Wilcoxon test was performed on the normalized grasp force, and the results are shown in Table 2. There was a significant difference between the free condition and the IMRL-L condition.
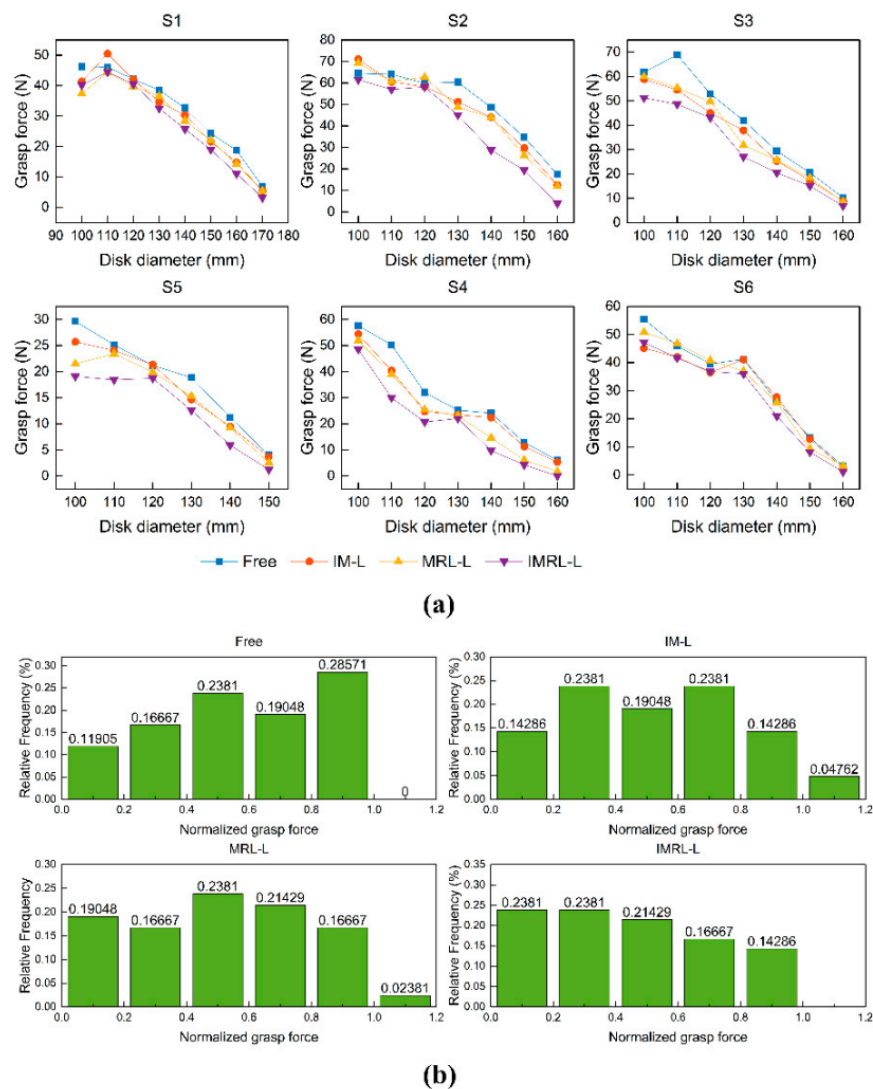

Figure 7. Results of the grasp force experiments. (**a**) Grasp force of 6 subjects, (**b**) frequency distribution histograms of normal grasp force under 4 conditions.

3.2. Grasping with a Simulator

The results of the simulated grasp are shown in Figures 8 and 9. In Figure 8, we show the maximum grasp quality out of 10 planning grasps of each constrained condition and disk diameter. The maximum evaluation of grasping under the free condition is significantly higher than that under the IM-L, MRL-L, and IMRL-L conditions except when the disc diameter is 120 mm. The particular case at 120 mm can be explained by the simulated annealing algorithm combining much randomness, leading to a probability event. In addition, it should be noted that except for the three grasping postures with an asterisk, the planned grasping postures all belong to the *precision disk* defined by Feix. For the hand whose ab/d DOF is restricted, the simulator had difficulty finding a way to grasp the disk with this posture as the diameter increased and was then forced to switch to the *extension* defined by Feix [30]. Such cases imply that ab/d DOFs could enable a superior grasp gesture to achieve a larger grasp workspace.
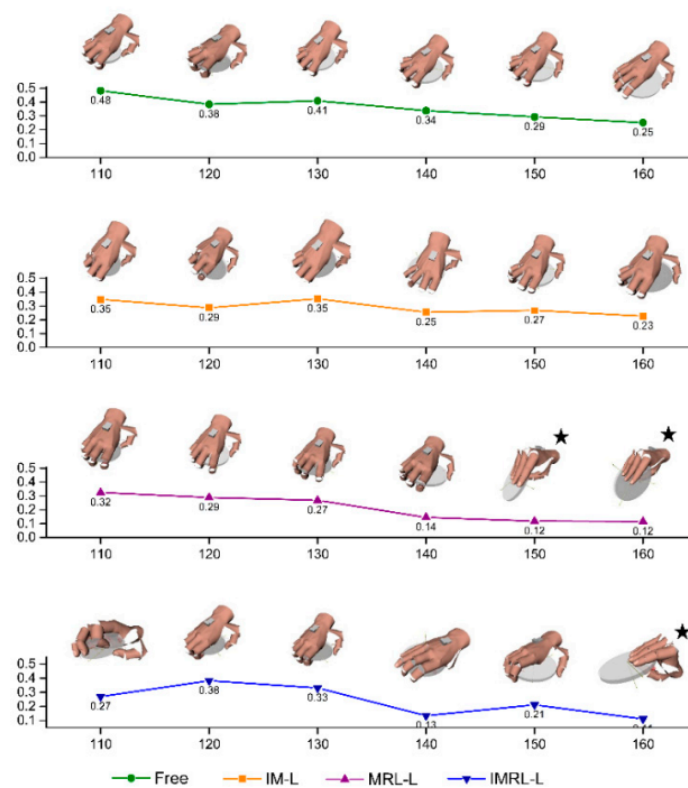

Figure 8. Maximum grasp quality with the simulator. The grasp gesture at each point is the optimal gesture out of 10 gestures. The asterisk represents an exceptive gesture that is not a *precision disk* grasp.

Each point in Figure 9 represents the average grasp quality of 10 superior grasping postures under four different conditions. The error bar is the standard deviation. We can see that the grasp quality under the free condition is significantly higher than that under the other three conditions, and the grasp quality under the IMRL-L condition is the lowest. Setting the average grasp quality under IMRL-L as a benchmark, the grasp quality under the previous three conditions increased by 76.7%, 50.1%, and 25.1%, on average. It is worth noting that when the disk diameter exceeds 130 mm, the grasp qualities under all four conditions exhibit sharp decreasing trends, indicating an increasing grasp difficulty as the object size increases.
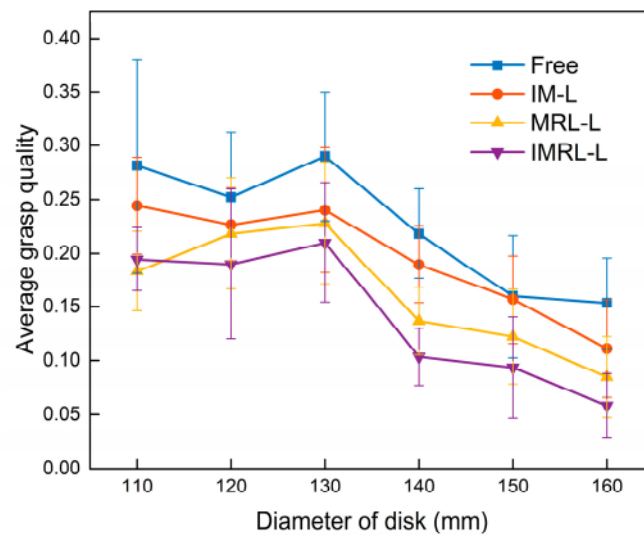
Figure 9. Average grasp quality with the simulator under 4 conditions.

3.3. Grasping with a Soft Robotic Hand

The results of grasping with a robotic hand are shown in Figure 10. The success rates of grasping with abduction are higher than those without abduction. The most significant difference was 80% (S4 and S5), while the smallest was 20% (S6). The total success rates were 51 out of 60 (with abduction) and 10 out of 60 (without abduction). The success rate was evaluated by the Wilcoxon test, as shown in Table 2. Comparisons of the grasp success rate with and without ab/d joints showed significantly different results.
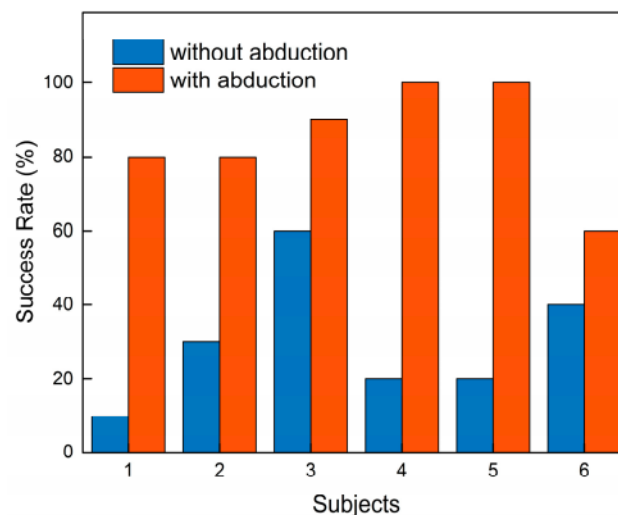

Figure 10. Comparison of grasping success rate with and without abduction of a soft robotic hand.

4. Discussion and Conclusions

A high priority in prosthetic hand design is the number of DOFs, which depends on the usage scenario, actuation method, control algorithm and so on [12,40]. Ab/d DOFs are frequently neglected in robotic hand design, especially for commercial prosthetic hands. In this paper, the effect of ab/d DOFs on grasping is studied. Experiments based on grasping a set of disks with various diameters by human hand, simulator, and robotic hand were conducted, which indicated that ab/d DOFs could distinctly promote the grasp size, grasp force, grasp quality, and grasp success rate. Furthermore, experimental results under four various conditions show that possessing at least one ab/d DOF can significantly improve

the performance of the prosthetic hand, which is consistent with the conclusion mentioned in [12,13] and can be applied to robotic hand design.

One of the crucial reasons that ab/d DOF promotes grasp size, force, quality and success rate is probably the more extensive active range of motion (ROM) of the fingers [41], enabling a larger grasp space and more dexterous contact points between fingers and objects. To further verify this, we studied the contact point under four conditions when grasping a disk with a diameter of 120 mm, whose size is close to a CD. A glove with markers attached to the fingertips was used (Figure 11a). The contact points during a tenfold grasp process were recorded, as shown in Figure 11b. We can see that the points under the free condition were most dispersive, possibly implying more stability during grasping, and the points under the IMRL-L condition were most centralized.
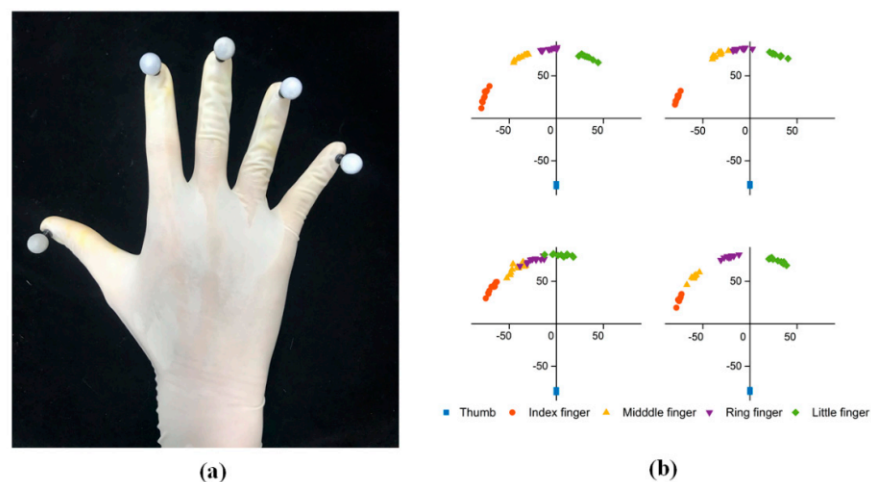

Figure 11. (**a**) A glove with markers can be captured by a motion tracking system; (**b**) contact point distribution of grasping a 120 mm diameter disk under four conditions. The unit of coordinate system is millimeters.

In addition, the size of objects may also influence the results of grasping. Intuitively, a larger object requires a larger grasp space so that having ab/d DOF is an advantage. In [42,43], the mean optimal handle diameter was calculated to be 38–40 mm. When the size of the grasped object exceeds this value, an increase in the object size leads to a reduction in the grasp force [43]. Six subjects carried out a Box and Block test [34] under four conditions to evaluate it. The results are shown in Figure 12. We can see that the numbers of blocks grasped per minute under the four conditions are basically equal because the blocks in this test are small (wood cubes with sides of approximately 24 mm). In this case, the grasp space brought by ab/d DOFs is redundant. However, Federico et al. showed that the complete free state of the MCP joint significantly improved the grasping operation with tasks involving a tripod grasp [12]. This may be caused by the fact that the operation after grasping is the key factor in some specific operations. Therefore, the flexibility of the MCP joint has advantages, even in grasping small objects.
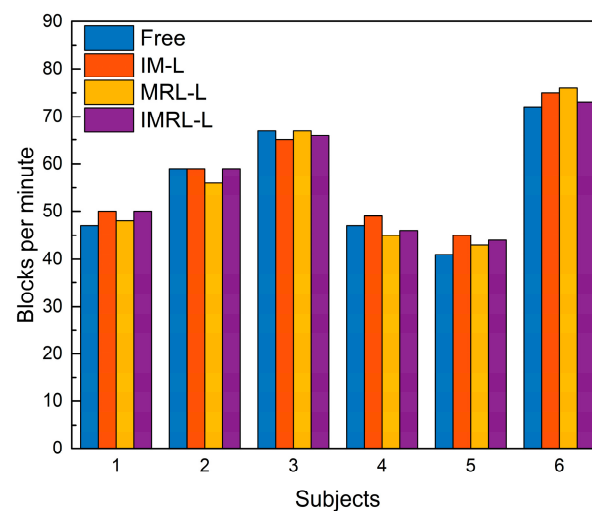
Figure 12. Experimental results of the Box and Block test.

5. Limitations and Future Work

This work still has some limitations. Grasping is a very complex operation that is affected by the shape and position of the object, the structure of the manipulator, the external environment and the purpose of using the object after grasping. It is far from sufficient to study the single grasp type of a single target. In addition, the sensitivity of the manipulator design based on different purposes to various parameters is also distinctive. In future work, we will expand the research goal and explore more objects and grasp types. In addition, in-hand manipulation is also a crucial operation type. The goal setting of such operations will also affect the design principle of the manipulator. It is necessary to study the dependence of in-hand manipulation on joint mobility in future work.

Author Contributions: Y.Y. and Y.W. conceived the idea and designed the study. Y.Y. and C.C. proposed the design of the experiments. Y.Y., M.G., J.Z. performed experiments and analyzed the experimental data. Y.Y. and C.C. coded the program and prepared the manuscript. All authors have read and agreed to the published version of the manuscript.

Institutional Review Board Statement: The experimental protocol was established according to the ethical guidelines of the Helsinki Declaration and was approved by the Human Ethics Committee of Beihang University.

Informed Consent Statement: Informed consent was obtained from all subjects involved in the study. Written informed consent was obtained from the patients to publish this paper.

Data Availability Statement: The datasets generated or analyzed during the current study are available from the corresponding author on reasonable request.

Conflicts of Interest: The authors declare that they have no competing interest.

References

1. Napier, J.; Tuttle, R.H. *Hands*; Princeton University Press: Princeton, NJ, USA, 1993.
2. Bullock, I.; Ma, R.; Dollar, A. *A Hand-Centric Classification of Human and Robot Dexterous Manipulation*; IEEE Computer Society Press: Los Alamitos, CA, USA, 2013.
3. Cooney, W.P.; Chao, E. Biomechanical analysis of static forces in the thumb during hand function. *J. Bone Jt. Surg. Am. Vol.* **1977**, *59*, 27–36. [CrossRef]
4. Li, Z.M.; Jie, T. Coordination of thumb joints during opposition. *J. Biomech.* **2007**, *40*, 502–510. [CrossRef] [PubMed]
5. Lin, H.T.; Kuo, L.C.; Liu, H.Y.; Wu, W.L.; Su, F.C. The three-dimensional analysis of three thumb joints coordination in activities of daily living. *Clin. Biomech.* **2011**, *26*, 371–376. [CrossRef] [PubMed]

6. Grebenstein, M. *Approaching Human Performance: The Functionality-Driven Awiwi Robot Hand*; Springer: Berlin/Heidelberg, German, 2014.

7. Youm, Y.; Gillespie, T.E.; Flatt, A.E.; Sprague, B. Kinematic investigation of normal MCP joint. *J. Biomech.* **1978**, *11*, 109–118. [CrossRef]

8. Gillespie, T.E.; Flatt, A.E.; Youm, Y.; Sprague, B.L. Biomechanical evaluation of metacarpophalangeal joint prosthesis designs. *J. Hand Surg.* **1979**, *4*, 508–521. [CrossRef]

9. Yuan, L.; Li, J.; Yang, D.; Yu, L.; Hong, L. Analysis on the joint independence of hand and wrist. In Proceedings of the 2016 IEEE International Conference on Advanced Intelligent Mechatronics, Banff, AB, Cananda, 12–15 July 2016.

10. Vinjamuri, R.; Mao, Z.H.; Sclabassi, R.; Sun, M.; Medicine, B.; Conference, B.S. Time-Varying Synergies in Velocity Profiles of Finger Joints of the Hand during Reach and Grasp. In Proceedings of the 2007 29th Annual International Conference of the IEEE Engineering in Medicine and Biology Society, Lyon, France, 23–26 August 2007; pp. 4846–4849.

11. Ergen, H.I.; Oksuz, C. Evaluation of Load Distributions and Contact Areas in 4 Common Grip Types Used in Daily Living Activities. *J. Hand Surg.* **2019**, *45*, 251-e1. [CrossRef]

12. Montagnani, F.; Controzzi, M.; Cipriani, C. Independent Long Fingers are not Essential for a Grasping Hand. *Sci. Rep.* **2016**, *6*, 35545. [CrossRef]

13. Zarzoura, M.; Del Moral, P.; Awad, M.I.; Tolbah, F.A. Investigation into reducing anthropomorphic hand degrees of freedom while maintaining human hand grasping functions. *Proc. Inst. Mech. Eng. Part H J. Eng. Med.* **2019**, *233*, 279–292. [CrossRef]

14. ShadowRobotCompany. *Design of a Dextrous Hand for Advanced CLAWAR Applications*; Shadow Robot Company: London, UK, 2003.

15. Deshpande, A.D.; Xu, Z.; Weghe, M.J.V.; Brown, B.H.; Ko, J.; Chang, L.Y.; Wilkinson, D.D.; Bidic, S.M.; Matsuoka, Y. Mechanisms of the Anatomically Correct Testbed Hand. *IEEE ASME Trans. Mechatron.* **2013**, *18*, 238–250. [CrossRef]

16. Belter, J.T.; Segil, J.L.; Dollar, A.M.; Weir, R.F. Mechanical design and performance specifications of anthropomorphic prosthetic hands: A review. *J. Rehabil. Res. Dev.* **2013**, *50*, 599–618. [CrossRef]

17. Cordella, F.; Ciancio, A.L.; Sacchetti, R.; Davalli, A.; Cutti, A.G.; Guglielmelli, E.; Zollo, L. Literature Review on Needs of Upper Limb Prosthesis Users. *Front. Neurosci.* **2016**, *10*, 209. [CrossRef]

18. Biddiss, E.A.; Chau, T.T. Upper limb prosthesis use and abandonment: A survey of the last 25 years. *Prosthet. Orthot. Int.* **2007**, *31*, 236–257. [CrossRef]

19. Liu, X.; Zhao, Y.; Geng, D.; Chen, S.; Tan, X.; Cao, C. Soft Humanoid Hands with Large Grasping Force Enabled by Flexible Hybrid Pneumatic Actuators. *Soft Robot.* **2021**, *8*, 175–185. [CrossRef]

20. Scharff, R.B.N.; Doubrovski, E.L.; Poelman, W.A.; Jonker, P.P.; Wang, C.C.L.; Geraedts, J.M.P. Towards Behavior Design of a 3D-Printed Soft Robotic Hand. In *Soft Robotics: Trends, Applications and Challenges*; Biosystems & Biorobotics; Springer: Cham, Switzerland, 2017; pp. 23–29.

21. Zhou, J.; Yi, J.; Chen, X.; Liu, Z.; Wang, Z. BCL-13: A 13-DOF Soft Robotic Hand for Dexterous Grasping and In-Hand Manipulation. *IEEE Robot. Autom. Lett.* **2018**, *3*, 3379–3386. [CrossRef]

22. Deimel, R.; Brock, O. A novel type of compliant and underactuated robotic hand for dexterous grasping. *Int. J. Robot. Res.* **2015**, *35*, 161–185. [CrossRef]

23. Zhao, H.; O'Brien, K.; Li, S.; Shepherd, R.F. Optoelectronically innervated soft prosthetic hand via stretchable optical waveguides. *Sci. Robot.* **2016**, *7*, eaai7529. [CrossRef]

24. She, Y.; Li, C.; Cleary, J.; Su, H.-J. Design and Fabrication of a Soft Robotic Hand with Embedded Actuators and Sensors. *J. Mech. Robot.* **2015**, *7*, 021007. [CrossRef]

25. Xu, Z.; Todorov, E. Design of a Highly Biomimetic Anthropomorphic Robotic Hand towards Artificial Limb Regeneration. In Proceedings of the 2016 IEEE International Conference on Robotics and Automation (ICRA), Stockholm, Sweden, 16–21 May 2016.

26. Ficuciello, F.; Pisani, G.; Marcellini, S.; Siciliano, B. The PRISMA Hand I: A novel underactuated design and EMG/voice-based multimodal control. *Eng. Appl. Artif. Intell.* **2020**, *93*, 103698. [CrossRef]

27. Festo. Festo_BionicSoftHand_en. Available online: https://www.festo.com/PDF_Flip/corp/Festo_BionicSoftHand/en/2-3/ (accessed on 10 October 2021).

28. Gracia-Ibáñez, V.; Sancho-Bru, J.L.; Vergara, M. Relevance of grasp types to assess functionality for personal autonomy. *J. Hand Ther.* **2018**, *31*, 102–110. [CrossRef]

29. Cutkosky, M. On grasp choice, grasp models, and the design of hands for manufacturing tasks. *IEEE Trans. Robot. Autom.* **1989**, *5*, 269–279. [CrossRef]

30. Feix, T.; Romero, J.; Schmiedmayer, H.-B.; Dollar, A.M.; Kragic, D. The GRASP Taxonomy of Human Grasp Types. *IEEE Trans. Hum.-Mach. Syst.* **2016**, *46*, 66–77. [CrossRef]

31. Cini, F.; Ortenzi, V.; Corke, P.; Controzzi, M.J.S.R. On the choice of grasp type and location when handing over an object. *Sci. Robot.* **2019**, *4*, eaau9757. [CrossRef]

32. Demers, L.A.A.; Gosselin, C. Kinematic Design of a Planar and Spherical Mechanism for the Abduction of the Fingers of an Anthropomorphic Robotic Hand. In Proceedings of the 2011 IEEE International Conference on Robotics and Automation, Shanghai, China, 9–13 May 2011.

33. Hill, W.; Kyberd, P.; Hermansson, L.N.; Hubbard, S.; Stavdahl, Ø.; Swanson, S. Upper Limb Prosthetic Outcome Measures (ULPOM): A Working Group and Their Findings. *J. Prosthet. Orthot.* **2009**, *21*, 69–82. [CrossRef]

34. Mathiowetz, V.; Volland, G.; Kashman, N.; Weber, K. Adult Norms for the Box and Block Test of Manual Dexterity. *Am. J. Occup. Ther. Off. Publ. Am. Occup. Ther. Assoc.* **1985**, *39*, 386–391. [CrossRef]

35. Miller, A.; Allen, P. GraspIt!: A versatile simulator for robotic grasping. *IEEE Robot. Autom. Mag.* **2005**, *11*, 110–122. [CrossRef]

36. Ciocarlie, M.; Goldfeder, C.; Allen, P. Dimensionality reduction for hand-independent dexterous robotic grasping. In Proceedings of the 2007 IEEE/RSJ International Conference on Intelligent Robots & Systems, San Diego, CA, USA, 29 October–2 November 2007.

37. Ciocarlie, M.T.; Allen, P.K. Hand Posture Subspaces for Dexterous Robotic Grasping. *Int. J. Robot. Res.* **2009**, *28*, 851–867. [CrossRef]

38. Ingber, L. Very fast simulated re-annealing. *Math. Comput. Model.* **1989**, *12*, 967–973. [CrossRef]

39. Yan, Y.; Wang, Y.; Chen, X.; Shi, C.; Yu, J.; Cheng, C. A tendon-driven prosthetic hand using continuum structure. In Proceedings of the 2020 42nd Annual International Conference of the IEEE Engineering in Medicine and Biology Society (EMBC), Montreal, QC, Canada, 20–24 July 2020; IEEE: Manhattan, NY, USA, 2020; Volume 2020, pp. 4951–4954.

40. Montagnani, F.; Controzzi, M.; Cipriani, C. Is it Finger or Wrist Dexterity That is Missing in Current Hand Prostheses? *IEEE Trans. Neural Syst. Rehabil. Eng.* **2015**, *23*, 600–609. [CrossRef] [PubMed]

41. Bain, G.I.; Polites, N.; Higgs, B.G.; Heptinstall, R.J.; Mcgrath, A.M. The functional range of motion of the finger joints. *J. Hand Surg.* **2015**, *40*, 406–411. [CrossRef]

42. Seo, N.J.; Armstrong, T.J. Investigation of grip force, normal force, contact area, hand size, and handle size for cylindrical handles. *Hum. Factors* **2008**, *50*, 734–744. [CrossRef]

43. Edgren, C.S.; Radwin, R.G.; Irwin, C.B. Grip Force Vectors for Varying Handle Diameters and Hand Sizes. *J. Hum. Factors Ergon. Soc.* **2004**, *46*, 244. [CrossRef]